EXIT-Chart Based Labeling Design for Bit-interleaved Coded Modulation with Iterative Decoding

Tsang-Wei Yu, Chu-Yan Wang, Chung-Hsuan Wang, and Wern-Ho Sheen
Department of Communication Engineering, National Chiao Tung University
Hsinchu, Taiwan 30056, R.O.C.
toshiba.cm93g@nctu.edu.tw, cywang.cm94g@nctu.edu.tw, chwang@mail.nctu.edu.tw, whsheen@mail.nctu.edu.tw

***Abstract*— In this paper, labeling is jointly designed with the outer code by the EXIT chart based analysis to improve the performance of bit-interleaved coded modulation with iterative decoding. A systematic design methodology is proposed for regular modulation schemes which can easily obtain a set of labelings with various slopes. Given an outer code, the optimal labeling which has the steepest slope but still makes the tunnel between the decoder and demapper transfer curves open can then be chosen to optimize the BER performance. Verified by the simulation results, our design can provide remarkable SNR gain over the conventional ones.**

I. Introduction

Bit-interleaved coded modulation (BICM) [1][2] is an efficient and powerful transmission scheme for fading channels, which comprises the serial concatenation of a conventional channel code (called the outer code) and a signal mapper (called the inner code) with a bit-wise interleaver inserted as in Fig. 1. Aided with the bit-wise interleaver, rich of diversity can be obtained by BICM to beat the channel impairments. However, such an interleaver also makes the optimal decoding of BICM infeasible. On account of the serially concatenated structure of BICM, BICM with iterative decoding (BICM-ID) which iteratively exchanges the soft-outputs between the demapper and the decoder was proposed in [3][4] to improve the decoding performance. With a proper labeling design of the signal constellation, BICM-ID has been shown to provide similar bit-error-rate (BER) performance to the optimal decoding for both of fading and non-fading channels.

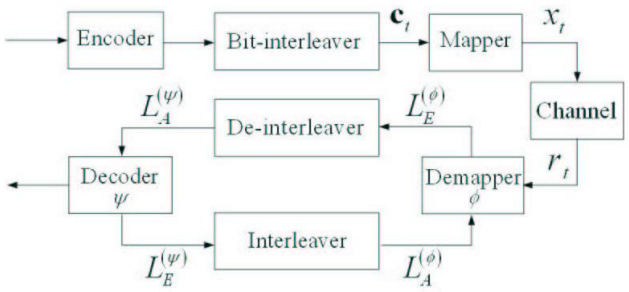

Fig. 1. Block diagram of BICM-ID systems.

To find out the optimal labeling for BICM-ID, the BER bounds [2] of BICM were further extended in [4]-[6] with the assumption of ideal feedback from the decoder. Their results suggest that the optimal labeling should maximize the minimum Euclidean distance between any pairs of modulated symbols which have only one distinct bit on their labels. In addition, labeling design based on the extrinsic information transfer (EXIT) chart [7] indicates that the optimal labeling should maximize the mutual information of demapper outputs as ideal a priori inputs from the decoder are assumed available [8]. Based on these criteria, various algorithms have been proposed in to search the optimal labelings for regular modulation schemes, e.g., phase-shift keying (PSK) and quadrature amplitude modulation (QAM) [5][6][8].

In terms of the EXIT chart, given an outer code, a good labeling should be designed to form a tunnel between the transfer curves of demapper and decoder at signal-to-noise ratio (SNR) as low as possible to guarantee a low threshold for BICM-ID. The demapper curve should also intersect the decoder curve at a point with mutual information as large as possible to avoid the undesired error floor at high SNR. However, labelings obtained in the previous researches are designed in spite of the outer code. The expected optimal performance hence can not always be achieved as different outer codes are employed. In most of the cases, those labelings perform well only at high SNR while unacceptable BER degradation is observed in the low SNR region. To improve the performance of BICM-ID, in this paper, labeling is jointly designed with the outer code by the EXIT chart based analysis. We observe that for regular modulation schemes the demapper curves associated with distinct labelings can be approximated to straight lines with a common intersection in the center of EXIT chart at low and moderate SNR. Stimulated by such a observation, a systematic methodology of labeling design is proposed for regular modulation schemes which can easily obtain a set of labelings (called the candidate set) with various slopes between the Gray labeling (with almost flat transfer curve) and the conventional optimal labeling (with the steepest slope). Given an outer code, we can then choose a labeling from the candidate set which is most matched to the outer code, i.e., the one with the steepest slope but still making the tunnel between the decoder and demapper curves open, to optimize the BER performance. Verified by the simulation results, our design can provide remarkable SNR gain over the conventional ones.

The rest of this paper is organized as follows. In Section II, a brief description of BICM-ID systems is given as well as the basic guideline of labeling design based on the EXIT chart. The systematic design methodology for optimal labeling is presented in Section III. In Section IV, simulation results are provided to verify the superiority of our design. Finally, a summary is drawn in Section V to conclude this work.

1-4244-1429-6/07/$25.00 ©2007 IEEE

II. System Model and EXIT Chart Based Analysis

A. System Model of BICM-ID

Consider the block diagram of BICM-ID systems in Fig. 1, where a constellation χ with M signal points x_0, x_1, $\cdots$, x_{M-1} is equipped with a labeling μ which assigns x_i a unique label $\mu(x_i)$ with $0 \leq \mu(x_i) < M \ \forall \ x_i$. Assume $M = 2^m$ for some positive integer m without loss of generality. Denote by $\boldsymbol{c}_t = (c_t^0, c_t^1, \ldots, c_t^{m-1})$ the coded bits after interleaving which are mapped to the modulated symbol s_t for transmission at time t. The received symbol corresponding to s_t can be represented by

$$r_t = \alpha_t s_t + n_t \tag{1}$$

where α_t denotes the channel gain at time t and n_t stands for the additive white Gaussian noise (AWGN) with zero mean and variance $N_0/2$ per dimension. The demapper ϕ takes r_t's and the a priori inputs $L_A^{(\phi)}(c_t^i)$'s, i.e., the feedback log-likelihood ratios (LLR) of c_t^i's from the decoder ψ, and then computes the extrinsic outputs by [6]

$$\begin{aligned} L_E^{(\phi)}(c_t^i) &= \ln \frac{\Pr(c_t^i = 1 | r_t)}{\Pr(c_t^i = 0 | r_t)} - L_A^{(\phi)}(c_t^i) \\ &= \ln \frac{\sum\limits_{x \in \chi_1^i} \exp\{-\frac{\|r_t - \alpha_t x\|^2}{N_0} + \sum\limits_{j \neq i} c_t^j L_A^{(\phi)}(c_t^j)\}}{\sum\limits_{x \in \chi_0^i} \exp\{-\frac{\|r_t - \alpha_t x\|^2}{N_0} + \sum\limits_{j \neq i} c_t^j L_A^{(\phi)}(c_t^j)\}} \end{aligned} \tag{2}$$

where χ_b^i is the subset of χ comprising all the signal points for those the i-th bit of the binary representation of their labels is of value b. Note that $L_E^{(\phi)}(c_t^i)$'s also depend on the choices of χ and μ. The output LLRs of demapper are then de-interleaved and serve as the a priori inputs $L_A^{(\psi)}(c_t^i)$'s of decoder. Finally, the extrinsic outputs $L_E^{(\psi)}(c_t^i)$'s of the decoder generated by an appropriate soft-input soft-output decoding algorithm, e.g. BCJR algorithm [14], are feedback to the demapper for next iteration of processing.

B. Design Guideline Based on EXIT Chart

The EXIT chart has been verified to be a powerful tool to understand the convergence behavior of iterative decoding schemes [7]-[9]. To trace the effect of μ on BICM-ID, we also use the EXIT chart for performance analysis on account of its iterative processing nature. For BICM-ID, the EXIT chart consists of two curves for both the demapper and decoder. Each curves describes how the mutual information between input LLRs and coded bits transfers to that between output LLRs and coded bits. Consider an example with trajectory in Fig. 2, where $(I_A^{(\phi)}, I_E^{(\phi)})$ and $(I_A^{(\psi)}, I_E^{(\psi)})$ denote the mutual information of input and output LLRs of the demapper and decoder, respectively. The trajectory shows how the mutual information actually transfers between the demapper and decoder. The first intersection between the demapper and decoder curves is then the farthest point that the trajectory may reach, which also tells the performance limit of this BICM-ID system.

Therefore, given an outer code, a good labeling should be designed to form a tunnel between the transfer curves of demapper and decoder at SNR as low as possible to guarantee a low threshold for BICM-ID. The demapper curve should also intersect the decoder curve at a point with $(I_A^{(\phi)}, I_E^{(\phi)})$ or $(I_A^{(\psi)}, I_E^{(\psi)})$ as large as possible to avoid the undesired error floor at high SNR. Consider the example in Fig. 3, where two channel codes: a convolutional code with generator matrix $(1 + D^2, 1 + D + D^2)$ and a rate-1/2 turbo code with constituent code $\left(1, \frac{1+D^2+D^3}{1+D+D^3}\right)$ are investigated with two kinds of labeling: Gray and anti-Gray [13] at $E_b/N_0 = 4$ dB in AWGN channel. Based on the above design guideline, Gray labeling is preferable to the turbo code while anti-Gray is more matched to the convolutional code.

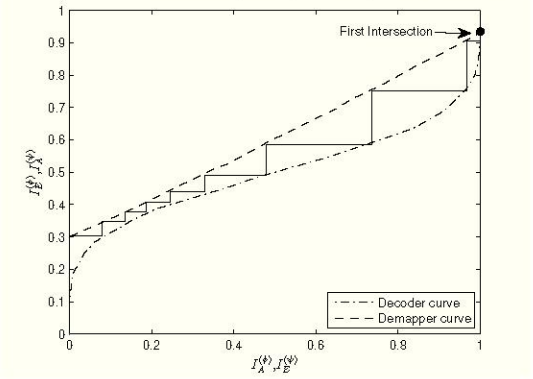

Fig. 2. An example of the EXIT chart for BICM-ID at $E_b/N_0 = 4$ dB in AWGN channel.

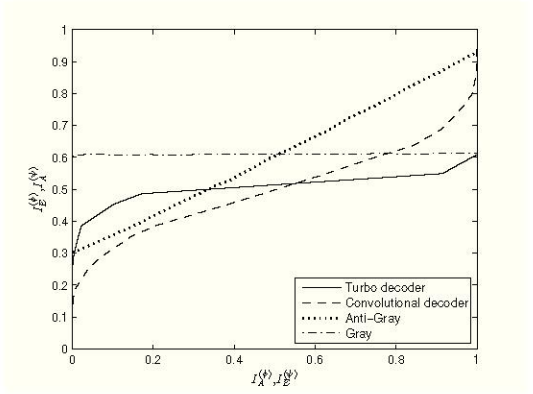

Fig. 3. EXIT chart for labeling design.

As observed from Fig. 3, a labeling may work well with some outer codes but performs poorly with others. Given the M-ary constellation, an intuitive way to find the optimal labeling with respect to some outer code is to plot the demapper curves of all possible $M!$ labelings and then choose the one most matched to the outer code. However, for a large M, the high complexity required for exhaustive search is usually far beyond what a practical system can afford. To provide a practical search scheme for the optimal labeling, a systematic design methodology with low search complexity is proposed in Section III.

III. New Design Methodology of Labeling with Low Search Complexity

For regular modulation schemes, e.g., PSK and QAM, we observe that the demapper curves corresponding to distinct labelings can be approximated to straight lines with a common intersection at low and moderate SNR. For instance, consider the demapper curves of the conventional labelings: Gray, Anti-Gray, Nature, SP [4], and Mixed [4] for BICM-ID with 16-QAM in Fig. 4. The straight-line approximation looks quite fit

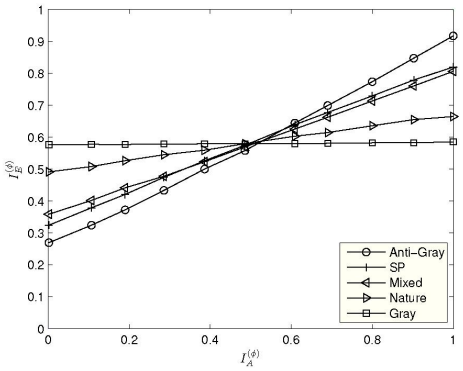

Fig. 4. Demapper transfer curves of some labelings for 16QAM at $E_b/N_0 = 3.5$ dB in AWGN channel.

for those curves, and a common intersection is also observed around the point with $I_A^{(\phi)} = 0.5$. For any labeling, the slope of its demapper curve can thus be determined by the maximum achievable $I_E^{(\phi)}$ with $I_A^{(\phi)} = 1$, denoted by I^*. In general, a labeling with a larger I^* can have a steeper transfer curve. In addition, given a constellation χ, consider two labelings μ_1 and μ_2 with $I_1^* << I_2^*$. For two signal points x_i and x_j in χ with $\mu_1(x_i) = \mu_2(x_j)$, suppose the labels of x_i and x_j in μ_1 are exchanged. We observe that the resulting new labeling can usually have a I^* larger than I_1^*. Moreover, the larger the Euclidean distance between x_i and x_j is, usually the larger increment of I^* is obtained.

Define $\mathcal{D} = \{d(x_i, x_j), \forall\ x_i, x_j \in \chi \text{ and } x_i \neq x_j\}$, where $d(x_i, x_j)$ is the Euclidean distance between x_i and x_j. Without loss of generality, assume the distinct distance d_i's in $\mathcal{D}$ are in an increasingly order, i.e., $d_i < d_j\ \forall\ i < j$. For example, consider 8-PSK with unit symbol energy; we have $\mathcal{D} = \{d_0, d_1, d_2, d_3\} = \{\sqrt{2-\sqrt{2}}, \sqrt{2}, \sqrt{2+\sqrt{2}}, 2\}$. Also, let μ^{-1} denote the inverse mapping of μ. Stimulated by the above significant observations, a systematic search procedure is proposed as follows which can easily obtain a set of labelings, called the candidate set Γ, with various slopes between two given labelings $\underline{\mu}$ and $\overline{\mu}$ with the flattest and steepest slopes, respectively.

Procedure for searching Γ:

Step 1: Set $\Gamma = \{\underline{\mu}, \overline{\mu}\}$, $\tilde{\mu} = \underline{\mu}$, $\hat{\mu} = \overline{\mu}$, and $k = 0$.
Step 2: For $0 \leq i < M$
  If $0 < d(\tilde{\mu}^{-1}(i), \hat{\mu}^{-1}(i)) \leq d_k$
    Swap the labels i and $\tilde{\mu}(\hat{\mu}^{-1}(i))$ in $\tilde{\mu}$ and set $\Gamma = \Gamma \bigcup \{\tilde{\mu}\}$.
Step 3: If $\tilde{\mu} \neq \hat{\mu}$
    Set $k = k + 1$ and go back to Step 2.
  Else Stop the procedure.

In the above procedure, labels of signal pair (x_i, x_j) with small Euclidean distance is exchanged first; $\tilde{\mu}$ can thus be updated with an incremental I^* in most of time, which implies an increment of the slope of demapper curve. However, there are at most M swaps of labels during each process of search, hence at most $M-1$ distinct new labelings are created in Γ. For a large M, Γ will finally contain sufficient labelings with slope in the range between those of $\underline{\mu}$ and $\overline{\mu}$. If M is small, we can reset $\tilde{\mu} = \overline{\mu}$ and $\hat{\mu} = \underline{\mu}$ in Step 1 and then initiate another search of Γ. In this way, new labelings with a decreasing slope different from those obtained previously may be searched. In addition, given a permutation π which defines an one-to-one and onto mapping from $\{0, 1, \cdots, M-1\}$ to $\{0, 1, \cdots, M-1\}$, Step 2 in the above procedure can be updated as the following:

Step 2: For $0 \leq i < M$
  If $0 < d(\tilde{\mu}^{-1}(\pi(i)), \hat{\mu}^{-1}(\pi(i))) \leq d_k$
    Swap the labels $\pi(i)$ and $\tilde{\mu}(\hat{\mu}^{-1}(\pi(i)))$ in $\tilde{\mu}$ and set $\Gamma = \Gamma \bigcup \{\tilde{\mu}\}$.

With different choices of π from the identity permutation, i.e., $\pi(i) = i\ \forall\ 0 \leq i < M$, we can also construct extra labelings which may not be obtainable in the original procedure.

Among the conventional labelings used for BICM-ID, Gray

TABLE I
CANDIDATE SET FOR 8PSK

μ for 8PSK	$(\mu(x_0), \mu(x_1), \ldots, \mu(x_7))$
SSP	(0,5,2,7,4,1,6,3)
A8	(0,5,7,2,4,1,6,3)
B8	(0,5,1,2,4,7,6,3)
C8	(3,0,1,2,7,6,5,4)
D8	(4,1,3,2,7,6,5,0)
E8	(1,0,3,2,7,6,5,4)
F8	(0,1,2,3,6,7,5,4)
Gray	(0,1,3,2,6,7,5,4)

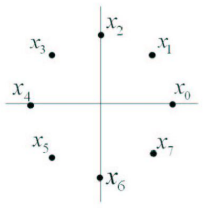

TABLE II
CANDIDATE SET FOR 16QAM

μ for 16QAM	$(\mu(x_0), \mu(x_1), \ldots, \mu(x_{15}))$
MSEW	(4,14,3,9,7,13,0,10,1,11,6,12,2,8,5,15)
A16	(0,14,3,9,4,11,7,10,1,13,15,12,8,2,5,6)
B16	(0,14,3,9,4,5,7,10,1,13,15,12,8,2,11,6)
C16	(4,12,3,2,7,5,0,15,1,11,6,14,9,8,13,10)
D16	(0,1,3,9,4,5,7,6,14,13,15,12,8,2,11,10)
E16	(4,1,3,2,0,5,7,15,12,11,6,14,9,8,13,10)
F16	(4,1,3,2,0,5,7,6,12,11,15,14,9,8,13,10)
G16	(4,1,3,2,0,5,7,6,12,13,15,14,9,8,11,10)
H16	(4,1,3,2,0,5,7,6,12,13,15,14,8,9,11,10)
Gray	(0,1,3,2,4,5,7,6,12,13,15,14,8,9,11,10)

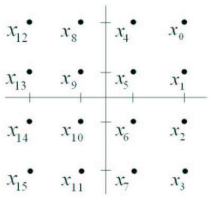

TABLE III
CANDIDATE SET FOR 64QAM

μ for 64QAM	$(\mu(x_0), \mu(x_1), \ldots, \mu(x_{63}))$
Anti-Gray	(17,47,50,4,49,13,42,29,15,32,21,41,2,62,25,19,24,23,34,30,53,9,38,56,51,8,31,48,11,55,12,3,5,40,63,36,10,61,0,59,44,27,6,58,37,22,43,16,7,5,60,33,14,57,20,45,28,54,1,26,52,3,46,18,39)
A64	(17,1,50,4,39,13,42,29,15,25,21,3,2,62,41,19,24,23,56,30,53,9,5,34,51,8,31,48,11,55,12,35,40,63,32,10,61,0,59,44,27,6,58,37,22,43,16,7,18,60,33,14,57,20,45,28,54,49,26,52,38,46,47,36)
B64	(17,1,50,4,6,13,5,29,15,9,21,3,2,62,7,19,24,23,56,30,53,0,14,28,51,8,31,48,11,55,12,47,40,63,16,10,61,25,59,44,27,39,58,37,22,49,54,60,18,41,33,42,57,20,45,34,32,43,26,52,38,46,35,36)
C64	(17,1,3,4,6,13,5,29,15,9,0,50,2,62,7,19,24,23,56,30,53,21,14,28,51,8,31,48,11,55,12,47,40,63,16,10,61,25,59,44,27,39,58,37,22,49,54,60,18,41,33,42,57,20,45,52,32,43,26,34,38,46,35,36)
D64	(17,1,3,4,6,13,5,29,0,9,15,50,2,62,7,21,24,25,56,30,53,19,14,28,51,8,31,48,11,55,12,47,40,49,16,10,61,23,26,44,27,39,58,37,22,63,54,60,18,41,33,42,57,20,45,52,32,43,35,34,38,46,59,36)
E64	(17,1,3,4,6,13,5,29,0,9,62,50,2,15,7,21,24,25,56,30,53,19,14,28,51,8,31,48,11,55,12,20,40,49,16,10,61,23,26,44,27,39,58,37,22,63,54,60,18,41,33,42,57,47,45,52,32,43,35,34,38,46,59,36)
F64	(17,1,3,14,6,13,5,29,0,9,62,50,2,15,7,21,24,25,56,30,53,19,4,28,51,8,31,18,11,55,12,20,40,49,16,10,61,23,26,44,27,57,58,37,22,63,54,60,48,41,33,42,39,47,45,52,32,43,35,34,38,46,59,36)
G64	(0,1,3,14,6,13,5,29,17,9,62,10,2,15,7,21,24,25,56,30,53,31,4,28,51,8,19,18,11,55,12,20,40,49,16,50,61,23,26,44,27,57,58,59,22,63,54,60,48,41,33,42,39,47,45,52,32,43,35,34,38,46,37,36)
H64	(0,1,3,14,6,13,5,4,17,9,62,10,2,15,7,12,24,25,27,30,53,31,29,28,51,8,19,18,11,55,21,20,40,49,16,50,61,23,26,52,56,57,58,59,22,63,54,60,48,41,33,42,39,47,45,44,32,43,35,34,38,46,37,36)
I64	(0,1,3,14,6,13,5,4,17,9,11,10,2,15,7,12,24,25,27,30,26,31,29,28,51,8,19,18,62,55,21,20,40,49,16,50,61,23,53,52,56,57,58,59,22,63,54,60,48,41,33,42,39,47,45,44,32,43,35,34,38,46,37,36)
J64	(0,1,3,14,6,13,5,4,17,9,11,10,2,15,7,12,24,25,27,30,26,31,29,28,51,8,19,18,22,55,21,20,40,49,16,50,54,23,53,52,56,57,58,59,62,63,61,60,48,41,33,42,39,47,45,44,32,43,35,34,38,46,37,36)
K64	(0,1,3,14,6,13,5,4,8,9,11,10,2,15,7,12,24,25,27,30,26,31,29,28,16,17,19,18,22,55,21,20,40,49,51,50,54,23,53,52,56,57,58,59,62,63,61,60,48,41,33,42,39,47,45,44,32,43,35,34,38,46,37,36)
L64	(0,1,3,14,6,7,5,4,8,9,11,10,2,15,13,12,24,25,27,30,26,31,29,28,16,17,19,18,22,23,21,20,48,49,51,50,54,55,53,52,56,57,58,59,62,63,61,60,40,41,33,42,39,47,45,44,32,43,35,34,38,46,37,36)
Gray	(0,1,3,2,6,7,5,4,8,9,11,10,14,15,13,12,24,25,27,26,30,31,29,28,16,17,19,18,22,23,21,20,48,49,51,50,54,55,53,52,56,57,59,58,62,63,61,60,40,41,43,42,46,47,45,44,32,33,35,34,38,39,37,36)

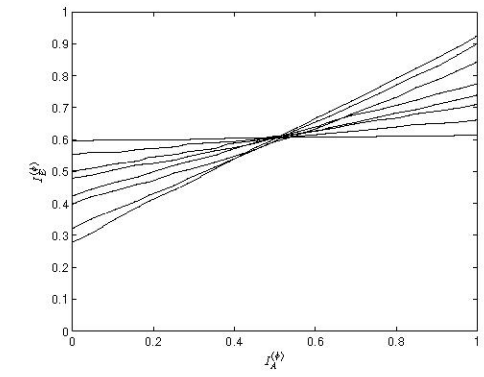

(a) Labelings for 8PSK in Table I

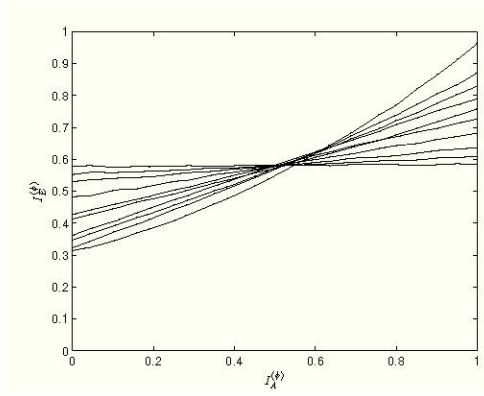

(b) Labelings for 16QAM in Table II

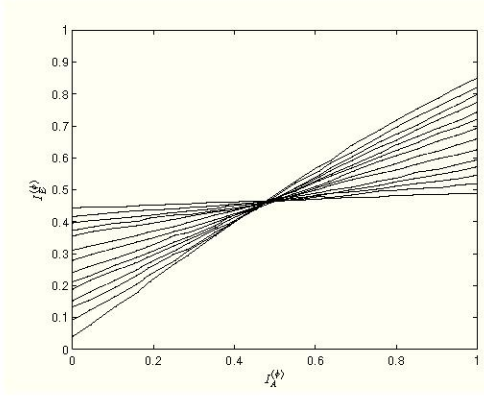

(c) Labelings for 64QAM in Table III

Fig. 5. Demapper transfer curves of labelings in Tables I,II,III.

labeling has a almost flat demapper curve while the others are designed in an optimal sense of making their slopes as steep as possible. For 8-PSK, 16-QAM, and 64-QAM, SSP [10], MSEW [11], and anti-Gray labelings are observed to have the steepest demapper curves, respectively. By choosing these labelings as $\underline{\mu}$ and $\overline{\mu}$ in the above procedure, the searched Γ's for 8-PSK, 16-QAM, and 64-QAM are presented in Tables I, II, III, where the labelings are listed in a decreasing order in terms of their slopes. (In Table III, the plot of signal constellation is omitted due to length limitation.) From Fig. 5, labelings in Γ are observed to generate the curves with slopes uniformly distributed between those of $\underline{\mu}$ and $\overline{\mu}$, where the curves are plotted in the same order as listed in Tables I, II, III with $E_b/N_0 = 3$ dB, 3.5 dB and 3.5 dB respectively. In addition, all the demapper curves can still keep the same order as in Fig. 5 at various SNRs. Therefore, given an outer code, we can then choose a labeling from Γ which has the steepest slope but still makes the tunnel between the decoder and demapper curves open to achieve both a low convergence threshold and acceptable BER at high SNR. Finally, only 28, 30, and 64 labelings are compared in the proposed procedure to obtain the Γ's for 8-PSK, 16-QAM, and 64-QAM, respectively; some labelings whose demapper curves with similar slope to those in Tables I, II, III are skipped. Compared with the exhaustive search which needs to investigate all of the 8!, 16!, and 64! labelings to find the optimal one for 8-PSK, 16-QAM, and 64-QAM, respectively, a large reduction of the search complexity is obtained here.

IV. Simulation Results

To verify the superiority of our design over the conventional labelings, the BICM-ID system consisting of a convolutional code with generator matrix $(1 + D^2 + D^3 + D^5 + D^6, 1 + D + D^2 + D^3 + D^6)$, a bit-interleaver of block length 24000 bits, and 8-PSK/16-QAM/64-QAM modulation is simulated for transmission over AWGN channels. The demapper in (2) and BCJR decoder of the outer code are employed for iterative decoding with 40 iterations. For 8-PSK modulation, conventional designs suggest MSEW and SSP with the steepest demapper curves as the optimal labelings for BICM-ID. However, at bit SNR (E_b/N_0) 3dB, the labeling that most matched the outer code in Table I is B8 as revealed from the EXIT chart in Fig. 6(a). From Fig. 6(a), the first intersection of the demapper and decoder curves for B8 is observed to have $I_E^{(\phi)}$ larger than which of Gray, MSEW and SSP; the tunnel between both curves opens for B8 but not for MSEW and SSP. Therefore, based on the guideline in Section II-B, B8 is expected to provide the best decoding performance, followed by Gray and then MSEW/SSP. The corresponding BER curves in Fig. 6(b) agree with the above analysis, which also show that our design can achieve 1.2 dB SNR gain over MSEW and SSP at BER 10^{-5}.

Similar observations can be obtained from the EXIT charts in Figs. 7(a), 8(a) and the BER curves in Figs. 7(b), 8(b). Among the labelings in Table II for 16-QAM, C16 outperforms the conventional designs: MSEW and M16a [12] with at least 0.75 dB SNR gain at BER 10^{-5}. For 64-QAM modulation, G64 in Table III even achieves a gain larger than 4 dB over anti-Gray at BER 10^{-5}. In fact, one can easily applies our design to other outer codes, e.g., turbo codes and low-density parity-check codes. The resulting gain is evident so that the related simulation results are omitted here.

V. Conclusions

A new design of labeling for BICM-ID is presented in this paper by the EXIT chart based analysis. We propose an efficient and systematic design methodology for regular modulation schemes which can easily obtain a set of labelings with various slopes. Given an outer code, the optimal labeling can be chosen from the searched set which has the steepest slope but still makes the tunnel between the decoder and demapper transfer curves open to optimize the decoding performance of BICM-ID. Verified by the simulation results, our design can provide remarkable SNR gain over the conventional ones.

References

[1] E. Zehavi, "Eight-PSK trellis codes for a Rayleigh channel," *IEEE Trans. Commun.*, vol. 40, pp. 873-884, May 1992.

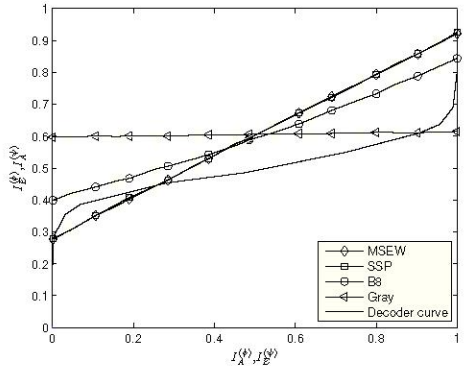

(a)

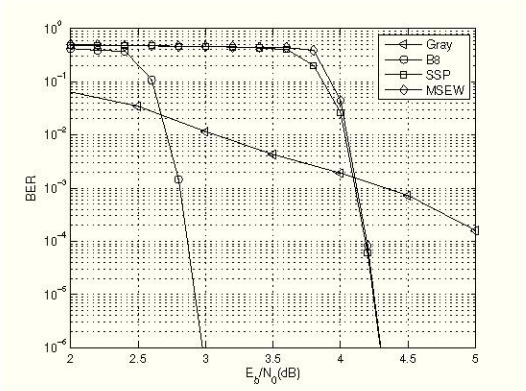

(b)

Fig. 6. (a) EXIT chart at $E_b/N_0 = 3$ dB and (b) performance plots of the BICM-ID system with 8PSK.

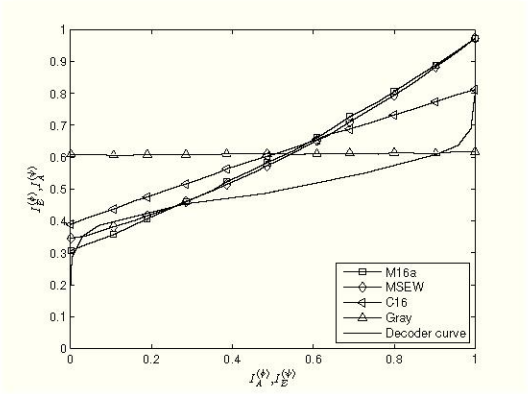

(a)

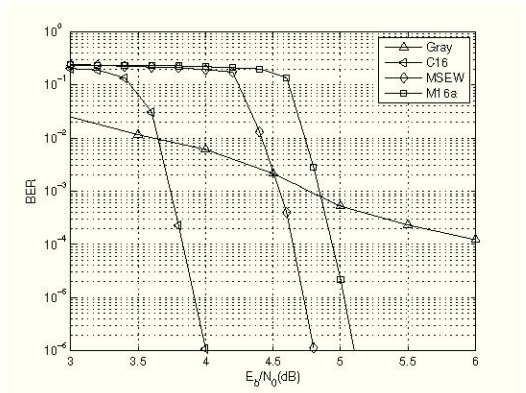

(b)

Fig. 7. (a) EXIT chart at $E_b/N_0 = 4$ dB and (b) performance plots of the BICM-ID system with 16QAM.

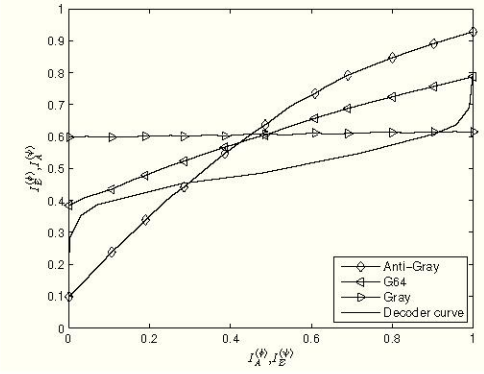

(a)

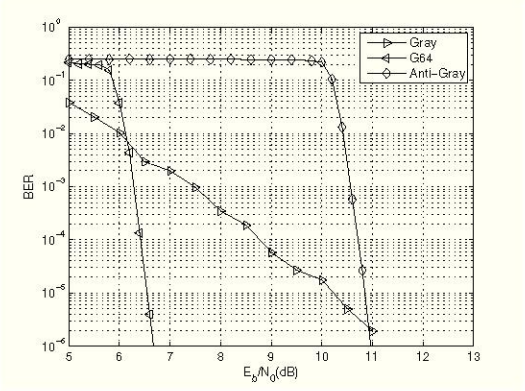

(b)

Fig. 8. (a) EXIT chart at $E_b/N_0 = 6.6$ dB and (b) performance plots of the BICM-ID system with 64QAM.

[2] G. Caire, G. Taricco, and E. Biglieri, "Bit-interleaved coded modulation," *IEEE Trans. Inform. Theory*, vol. 44, pp. 927-945, May 1998.

[3] X. Li and J. A. Ritcey, "Trellis coded modulation with bit interleaving and iterative decoding", *IEEE J. Select. Areas Commun.*, vol. 17, pp.715-724, 1999.

[4] A. Chindapol and J. A. Ritcey, "Design, analysis, and performance evaluation for BICM-ID with square QAM constellations in Rayleigh-fading channels", *IEEE J. Select. Areas Commun.*, vol. 19, pp. 944-957, May 2001.

[5] Y. Li and X. G. Xia, "Constellation mapping for space-time matrix modulation with iterative demodulation/decoding," *IEEE Trans. Commun.*, vol. 53, pp. 764-768, May 2005.

[6] Y. Huang and J. A. Ritcey, "Optimal constellation labeling for iteratively decoded bit-interleaved space-time coded Modulation," *IEEE Trans. Inform. Theory*, vol. 51, pp. 1865-1871, May 2005.

[7] S. ten Brink, "Convergence of iterative decoding," *Electron. Lett.*, vol. 35, pp. 806-808, May 1999.

[8] A. Sezgin and E. A. Jorswieck, "Impact of the mapping strategy on the performance of APP decoded space-time block codes," *IEEE Trans. Signal Process.*, vol. 53, pp. 4685-4690, Dec. 2005.

[9] S. ten Brink, "Convergence behavior of iteratively decoded parallel concatenated codes," *IEEE Trans. Commun.*, vol. 49, pp. 1727-1737, Oct. 2001.

[10] X. Li, A. Chindapol, and J. A. Ritcey,"Bit-interleaved coded modulation with iterative decoding and 8PSK signaling," *IEEE Trans. Commun.*, vol. 50, pp.1250-1257, Aug. 2002.

[11] J. Tan and G. L. Stuber, "Analysis and design of symbol mappers for iteratively decoded BICM," *IEEE Trans. Wireless Commun.*, vol 4, pp. 662-672, Mar. 2005

[12] F. Schreckenbach, N. Gortz, J. Hagenauer, and G. Bauch, "Optimization of symbol mappings for bit-interleaved coded modulation with iterative decoding," *IEEE Commun. Lett.*, vol 7, no 12, pp. 593-595, Dec. 2003

[13] A. Boronka and J. Speidel, "A low complexity MIMO system based on BLAST and iterative Anti-Gray-demapping," in *Proc. IEEE PIMRC 2003*, Beijing, China, Sept. 2003, pp. 1401-1404.

[14] L. R. Bahl, J. Cocke, F. Jelinek, and J. Raviv, "Optimal decoding of linear codes for minimizing symbol error rate," *IEEE Trans. Inform. Theory*, vol. 20, pp.284-287, Mar. 1974.